Lasers in Manufacturing Conference 2013

High precision surface structuring with ultra-short laser pulses and synchronized mechanical axes

B. Jaeggi[a]*, B. Neuenschwander[a], T. Meier[b], M. Zimmermann[b], G. Hennig[c]

[a]Bern University of Applied Sciences, Institute for Applied Laser, Photonics and Surface Technologies, Pestalozzistrasse 20, CH-3400 Burgdorf, Switzerland
[b]Bern University of Applied Sciences, Institute for Mechatronic Systems, Pestalozzistrasse 20, CH-3400 Burgdorf, Switzerland
[c]Daetwyler Graphics AG, Flugplatz, CH-3368 Bleienbach, Switzerland

Abstract

For surface and 3D structuring in a 2.5D process, ultra-short pulsed laser systems are mostly used in combination with mechanical axes, whereas the mechanical axes can include electrical motor as well as beam deflecting systems like a galvo scanner. The motion of the axes is synchronized with the clock of the laser pulses, by a modification of the electronic axes control. This work shows the scalability of the ablation process up to MHz-regime in relation to surface quality and ablation efficiency, drilling of thin foils without any heat accumulation and deforming problems of the foil. Furthermore the transfer of the machining strategy from a synchronized galvo scanner to a rotating cylinder setup is shown.

1. Introduction

A standard process for surface structuring applications is the 2.5D processing (fig. 1). The 3D structure is divided into several slices, with a given outline. This outline is filled with a parallel hatching. The lines of the hatch pattern are generated with mechanical axes, usually galvo scanners, and the laser pulse train is switched

---

* Corresponding author. Tel.: +41-34-4264193; Fax: +41-34-4231513.
E-mail address: beat.jaeggi@bfh.ch

on and off via an external modulator which is gated by a signal from the axes control software. Different situation at the border of a structure can appear. If the pulse train is switched on with the start of the
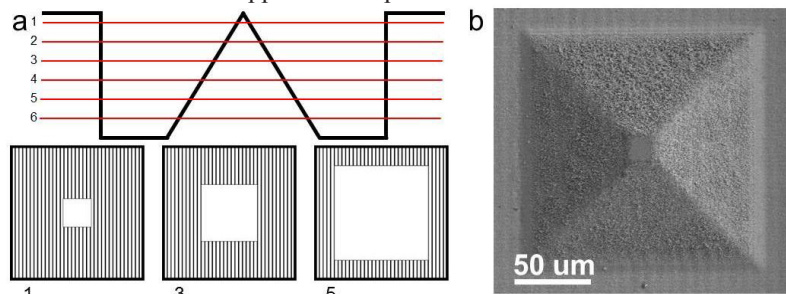

Fig. 1. 2.5D process (a) 2D slices; (b) SEM image of a 3D structure machined in Copper
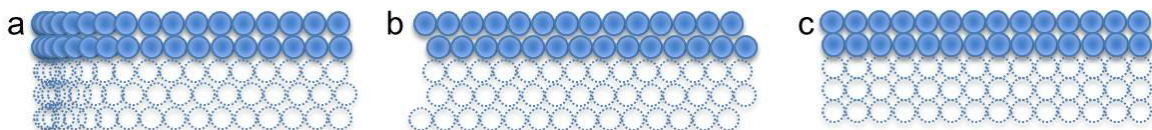

Fig. 2. Start positions of the different strategies: (a) without sky-writing; (b) with sky-writing; (c) synchronized system

axes acceleration the distance from pulse to pulse (pitch) increases until the axes has reached its final speed (fig. 2a). Such lines show deep marks at the start and ending points of the single lines but the effective position of these points are well defined. To avoid the phenomenon of deep marking a so called sky-writing option can be used. Sky-writing means that the axes already have the correct velocity at the beginning of the marking. With sky-writing option a displacement of the start position of plus/minus the distance between two consecutive pulses has to be accepted (fig. 2b). Therefore for high precision structuring applications this combination suffers from inaccuracies due to the asynchronous motion of the axes relative to the pulse train. If this problem should be avoided it will be necessary to synchronize the axes motion onto the output pulse train of the laser system or vice versa (fig. 2c). In the case of a Q-switched laser system the pulse train can be shifted by the external control software. This is a simple solution and is e.g. supported by many scanner control software. Currently in industrial applications ultra-short pulsed laser systems will be used if high requirements concerning accuracy, defined surface roughness and small heat affected zone are demanded. Unfortunately with Q-switched laser system the achievable pulse durations are not short enough for precise micro-processing. The today available industrially suited ultra-short pulsed systems are turnkey systems, set up in a master oscillator power amplifier (MOPA) arrangement with a passively mode locked seed laser, followed by a pulse picker and a rod or disk amplifier to prepare the output pulse train. However, a MOPA design has at the beginning of the amplifier chain a passively mode locked seed laser. The shift of the laser pulse train is a non-common task for industrial standard MOPA systems. Finally one has to tune the gating module and the followed mechanical components on the laser pulse train, meaning the laser is set up as a Master and the axes are the Slave-module.

In a first task the best machining strategy with respect to minimum surface roughness and structure dimension was investigated by using the synchronized galvo scanner. With repetition rates in the range of 100 kHz to 300 kHz and 532 nm wavelength we have shown in Jaeggi et al., 2012 the advantages and possibilities of the synchronized machining. On a polished copper target a minimum surface roughness of 90 nm *Ra*-value was achieved, machined with a pitch of half of the spot radius w_0. The minimum structure dimension which could be achieved was in the range of one spot radius. The structures were obtained by generating the corresponding bitmaps for each slice and working with the normal 2.5D process and random distributed starting values for each slice. As input serve greyscale images, which are divided into several black and white images by using a

threshold value for the greyscale value. Otherwise x-y-z-data serve as input by using a threshold for the height-value. If no change of the structure depth is needed, only one black and white image is used several times. To increase the competitiveness of micromachining with ultra-short laser pulses the process time i. e. the throughput is one of the key factors. For fast micromachining a fast deflection system is needed. With the galvo scanner we use a feed rate of 8 m/s. This speed needs a repetition rate in the MHz-regime in order to have an overlapping of the consecutive pulses. We show in this work the scalability of the process by linear increasing the repetition rate up to 1 MHz, the average power and the marking speed. Additionally by using a rotating sample like a rotating cylinder even higher processing speeds can be achieved. The transfer of the machining strategy from the galvo scanner to the rotation setup and the using of 2 MHz repetition rate are shown, as well. In industrial applications such cylinders can be used as embossing-rolls.

2. Experimental Setup

All experiments were performed with a DUETTO system (Time Bandwidth Products) generating 10 ps pulses at 1064 nm and 532 nm wavelength with repetition rates from 50 kHz to 8.2 MHz. The laser light was always circular polarized by using a λ/4-waveplate. The laser pulse train was monitored with an internal photodiode and the exact repetition rate and phase of the pulse train were electronically deduced. These were fed to an own developed control software synchronizing the motion of the galvo-mirrors and the axes of the rotating cylinder. With the synchronized set-up the machining strategy was changed from vector-scanning to a pixel representation where one pixel represents one "laser-shot" during the motion of the axes which is already shown in Jaeggi et al., 2012. Basic black and white bitmaps serve as input for the control software. In a first experiment the scalability of the process was tested on a flat sample using a synchronized galvo scanner (fig. 3) for deflecting the laser beam. As machining strategy the best strategy, which was found in previous experiments shown in Jaeggi et al., 2012, was used. The machining of small flat samples gives the possibility to analyze them with different microscopes like an SEM.

For ablation with a Gaussian beam at a certain peak fluence the ablation process is most efficient as shown in Raciukaitis et al., 2009 and Neuenschwander et al., 2010. This peak fluence depends on the threshold fluence which is for Copper, 512 pulses applied and a wavelength of 532 nm 0.11 J/cm2 and 0.31 J/cm2 for 1064 nm respectively. The energy penetration depth is 6.67 nm for 532 nm and 31.7 nm for 1064 nm. The peak fluence was chosen for all experiments to work close to this optimum point. With the used spot radii this leads in case of the synchronized scanner to pulse energies of 0.41 μJ for 532 nm and 9.2 μJ for 1064 nm. For the rotating cylinder the used pulse energy was 0.2 μJ due to the smaller spot radius compared to the galvo scanner. Therefore the maximum useable repetition rate, where the pulse energy is sufficient for ablating, is higher. To work at the point where the ablation process is most efficient a specific peak fluence has to be used. By increasing the repetition rate, also the average power has to be increased. This is insofar possible as the limit of the laser system is reached concerning the average power. Until this limit is reached, the unique factor to increase the repetition rate again, is to reduce the spot radius by changing the focal optic.
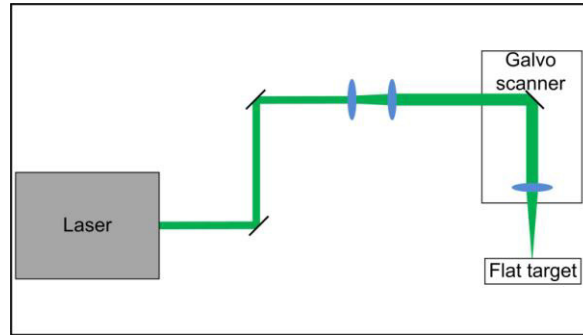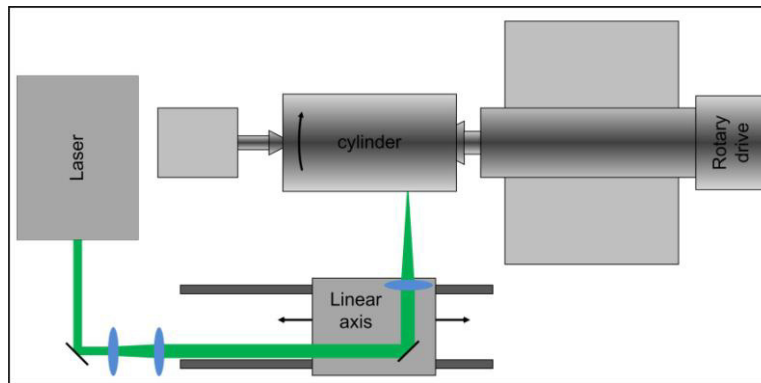
Fig. 3. Galvo scanner setup

Fig. 4. Setup to machine a rotating cylinder

At the same average power the maximum achievable repetition rate is higher for a smaller spot radius. The used scanner system was an IntelliScan$_{de}$14 with a 100 mm telecentric objective for 532 nm and a 160 mm f-theta objective for 1064 nm. The spot radius $w0$ was 5.7 μm for 532 nm and 16.3 μm for 1064 nm, respectively, and the beam quality $M2$ was smaller than 1.3, both measured with a slit scanning beam profiler.The sample material was copper Cu-DHP (in US: C12 200) whose surface was polished with a 3 μm diamond suspension. For the drilling tests, a 10 μm thick 1.4310 (in US: AISI 301) steel foil is used.

Due to the used objectives, the maximum used repetition rate amounts 1 MHz. In order to go to higher repetition rates a second experiment structuring a cylinder surface was performed using one rotation and one linear axis, which both were synchronized on the laser pulse train (fig. 4). The diameter of the cylinder was 150 mm and the wavelength of the processing laser was of 532 nm. The laser beam was focused with a lens with a focal length of f = 75 mm resulting in a spot radius of $w0$ of 4 μm and a beam quality $M2$ smaller than 1.3. With this spot radius repetition rates up to 2MHz could be tested on the cylindrical set up. The machined cylinder is a steel cylinder with an electro-plated copper coating.

3. Experimental Results

3.1. Synchronized galvo scanner

Fig. 5 shows a sequence of machined Tux, the icon of Linux in copper with 1064 nm using the 2.5D processing method with 100 different layers based on the image, found at the webpage of wikipedia.org of the Wikimedia Foundation Inc. The repetition rate was increased form 200 kHz (fig. 5a) to 1 MHz (fig. 5d). To

work at the optimum point, for 1 MHz repetition rate an average power of 9.25 W is needed. Due to the limit of the laser system the average power was 8.6 W instead of the 9.25 W. If heat accumulation occurs, the surface quality will decrease with increasing repetition rates. Comparing the SEM images in fig. 6, no decrease of the surface quality is observed for the increasing repetition rates. The small melting worms on the surface are for all repetition rates on the same scale, so the heat accumulation has no influence. Similar results concerning the influence of heat accumulation have been seen at the wavelength of 532 nm and repetition rates up to 1 MHz as shown in fig. 7. Another way to analyze the scalability of the process is the comparison of the depths of the structures. If particle shielding as shown in König et al., 2004 and Ancona et al., 2008 take place, a significant reduce of the structure depth with increased repetition rate should be observed. A comparison of the achieved structure depths shows no significant differences between low and high repetition rates. The depth are 25.2 um for 100 kHz and 28.92 μm for 1 MHz in case of 1064 nm wavelength and 16.75 μm for 300 kHz and 15.69 μm for 1 MHz in the case of 532 nm, respectively. With the used machining
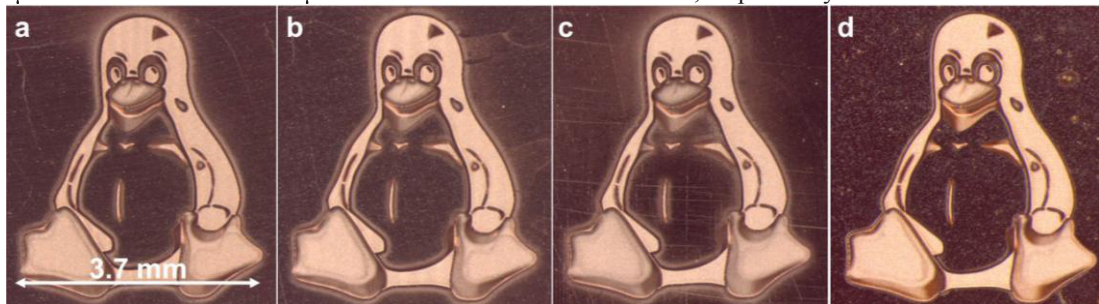

Fig. 5. Sequence of machined Tux with 1064 nm wavelength (a) 200 kHz, 1.8 W, 1.6 m/s; (b) 300 kHz, 2.8 W, 2.4 m/s; (c) 500 kHz, 4.6 W, 4 m/s; (d) 1 MHz, 8.6 W, 8 m/s
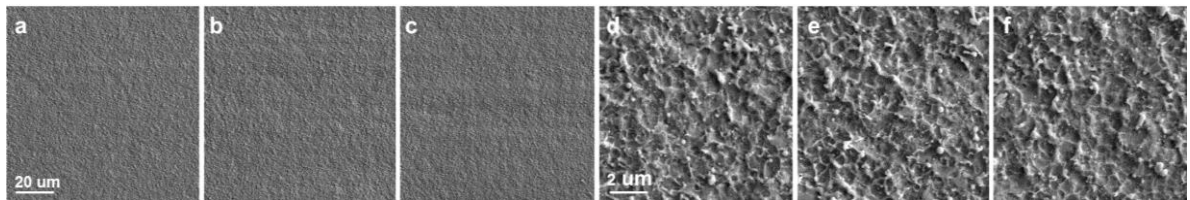

Fig. 6. SEM images of the surface quality of the Tux (a) 200 kHz; (b) 500 kHz; (c) 1 MHz, (d) Detail view of a; (e) Detail view of b; (f) Detail view of c
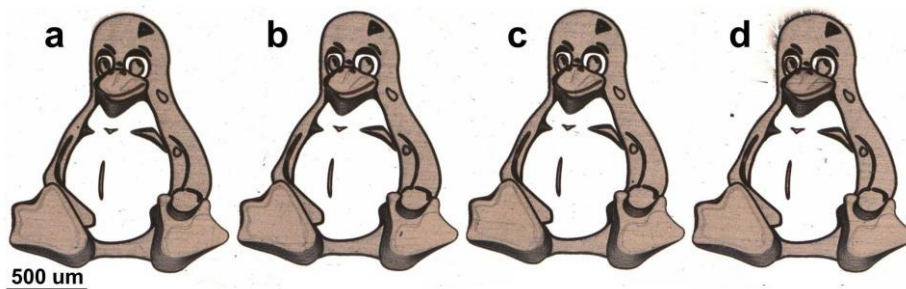

Fig. 7. Sequence of Tux machined with 532 nm wavelength (a) 300 kHz, 120 mW, 0.9 m/s; (b) 500 kHz, 204 mW, 1.5 m/s; (c) 700 kHz, 280 mW, 2.1 m/s; (d) 1 MHz, 408 mW, 3 m/s

strategy, the limit of the repetition rate, where the heat accumulation and/or the particle shielding have a strong influence, was not reached. Therefore the scalability of the ablation process by changing the repetition

rate up to 1 MHz is proofed. The high accuracy concerning the position during full motion of the scanner is shown in fig. 8. During one layer one pulse per cavity appears and it is clearly seen in the detail view (fig. 8c,d), that all 30 pulses strikes on the same point even at a speed of 8 m/s.
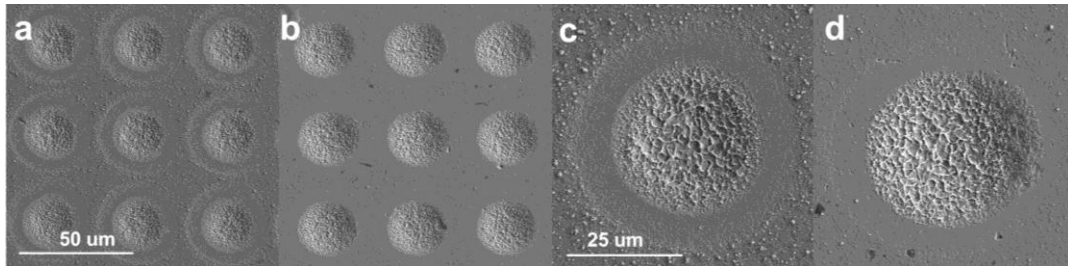

Fig. 8. Positioning accuracy (a) 200kHz; (b) 1MHz; (c) Detail view of a; (d) Detail view of b
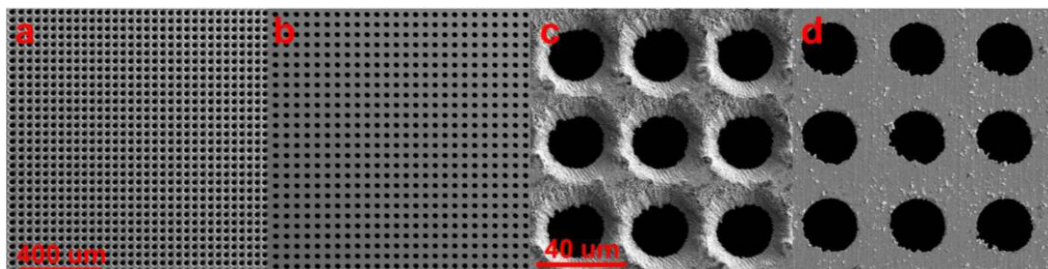

Fig. 9. Drilling on the fly through a 10 µm steel foil (a) Inlet; (b) Outlet; (c) Detail view of a; (d) Detail view of b

In a next step holes are drilled into a 10 µm thick steel foil using the percussion drilling method which is shown in Ancona et al., 2008. The deforming of thin foils due to heat is a well-known problem. This appears by using percussion drilling with a too high repetition rate. To exclude the heat accumulation, the repetition rate should be decreased but then the processing time increases and the process is no longer competitive. Another option is percussion drilling on the fly. Using the synchronized pixel represented machining during one slice only one pulse appears per hole. Therefore the frequency with which the pulses appear at the same spot is low and the deforming problem is excluded. The repetition rate of the laser itself is high to use a marking speed of several m/s. Fig. 9 shows the inlet and the outlet of holes drilled in a 10 µm thick steel foil with 1.64 W average power at 200 kHz repetition rate with a wavelength of 1064 nm. The scan speed was 8 m/s. The hole-arrangement is very periodically with a hole-spacing of 40 µm.

3.2. Rotating cylinder

The discovered strategy is transferred from a flat sample to a rotating cylinder where the higher speeds offered the possibility to work with repetition rates higher than 1 MHz. With this setup it is possible to strike the same position on the cylinder during the motion with an accuracy of about 1 µm up to a repetition rate of 2 MHz as shown in fig. 10a. The rotation speed of the cylinder was 8.5 rps which correlate to a relative slow surface speed of 4 m/s due to the small spot size. Red marked cavities in fig. 10a were shot twice and the other only once with an average power of 0.6 W at a repetition rate of 2 MHz. The next step is to machine a 3D structure as shown in the fig. 10b and 10c. In order to use the same machining strategy it is necessary to have the random distribution of the starting points as used in Jaeggi et al., 2012. Therefore during the backwards motion of the linear stage to the starting point of the new layer, the rotary motion is delayed for this random starting value. The inner part of the two squares in fig. 10b consists of 60 layers whereas the outer part only consists of 30 layers. The checkerboard pattern in fig. 10c consists of 30 layers. The black and white

images are the same for each slice, only the starting points are different. Other examples are shown in fig. 11. To machine the rose (fig. 11a) one black and white bitmap, which was found at the webpage zazzle.ch of Zazzle.com, Inc., is used ablating it 30 times. The next step is to machine a greyscale image, which is divided into 100 different black and white images, like the Tux, shown in fig. 11b. Fig. 11c shows a coherent checkerboard pattern, which is marked around the cylinder without any optical effects at the intersection marked in the image.
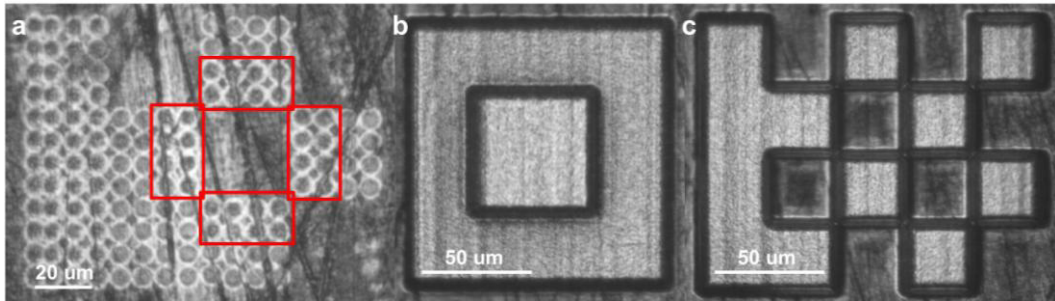

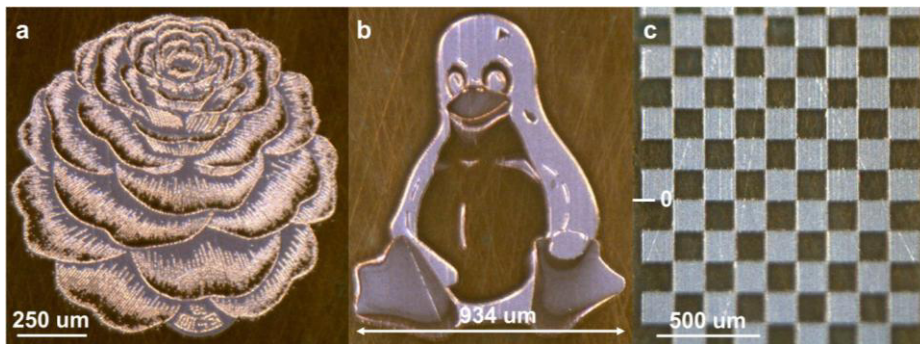Fig. 10. Structures on the cylinder (a) dnfjd; (b) dnffn; (c) dkfdk

Fig. 11. Structures on the cylinder a) dfd; (b) nfjdnfj; (c) djfkjd

4. Summary and Outlook

In a first step with the galvo scanner setup, the scalability of the machining process was demonstrated by linearly increasing the repetition rate, the average power and the marking speed up to 8 m/s in the case of 1064 nm and 3 m/s for 532 nm, respectively. No difference of the surface quality is observed between the different average powers. Also the ablation efficiency is nearly constant. In case of the used machining strategy, the heat accumulation and the particle shielding do not take place for repetition rates up to 1 MHz. Additionally we have shown that it is possible to machine a rotating cylinder with synchronized rotating and linear axes. The machining strategy can be transferred from the synchronized galvo scanner to the rotating cylinder. For both setups it is possible to strike the same point twice during full motion of the mirrors or the axes. This positioning accuracy opens the opportunity for drilling on the fly of thin heat-sensitive foils. A 10 μm steel foil is drilled without any heat accumulation and deforming.

For the cylinder setup in future the next step is to change the wavelength from 532 nm to 1064 nm and to enlarge the spot radius. Due to this increase of the spot radius the mark speed increases as well. These two factors lead to an average power in the range of 10 W and a repetition rate between 2 and 3 MHz. With the industrially suited laser system this repetition rates are the limit where the AOM can pick single pulses. To operate with single shots and higher repetition rates i.e. some MHz, the optical setup of the AOM has to be

changed. But then the minimum repetition rate of the laser system is in the MHz range due to the high peak fluences at repetition rates of some kHz in the AOM and its damage threshold. The introduction of an additional fast deflector as a third synchronized axis as used in Bruening et al., 2011, offers new opportunities to decrease the process time and will allow to use even higher average powers of several 10 W by increasing the repetition rate and the fast deflection. These high powers are achievable by using the same laser system with an additional amplifier.

Acknowledgements

References

Jaeggi B., Neuenschwander B., Hunziker U., Meier T., Zimmermann M., Hennig G. et al., 2012. "Ultra-high-precision surface structuring by synchronizing a galvo scanner with an ultra-short-pulsed laser system in MOPA arrangement," Proc. SPIE 8243

Jaeggi B., Neuenschwander B., Hunziker U., Zuercher J., Meier T., Zimmermann M. et al., 2012. "High precision and high throughput surface structuring by synchronizing mechanical axes with an ultra short pulsed laser system in MOPA arrangement," paper M1207, ICALEO

Raciukaitis G., Brikas M., Gecys P., Voisiat B., Gedvilas M., 2009. "Use of High Repetition Rate and High Power Lasers in Microfabrication: How to keep Efficiency High?," JLMN Journal of Laser Micro/Nanoengineering; Vol. 4 (3), p. 186

Neuenschwander B., Bucher G., Hennig G., Nussbaum C., Joss B., Muralt M., Zehnder S. et al., 2010. "Processing of dielectric materials and metals with ps laserpulses," ICALEO 2010, Paper M101

Neuenschwander B., Bucher G., Nussbaum C., Joss B., Muralt M., Hunziker U. et al., 2010. "Processing of dielectric materials and metals with ps-laserpulses: results, strategies limitations and needs," Proceedings of SPIE vol. 7584

Wikimedia Foundation Inc., 2001. Retrieved 31, January, 2013, http://en.wikipedia.org/wiki/File:Tux.svg

König J., Nolte S., Tünnermann A., 2005. "Plasma evolution dring metal ablation with ultrashort laser pulses," Opt. Express, Vol. 13, p. 10597

Ancona A., Röser F., Rademaker K., Limpert J., Nolte S. and Tünnermann A., 2008. "High speed laser drilling of metals using a high repetition rate, high average power ultrafast fiber CPA system," Opt. Express, Vol. 16, p. 8958

Zazzle.com, Inc., 2000. Retrieved 31, January, 2013, http://www.zazzle.ch/rosen_lithographie_fotoskulptur-153582013095294502

Bruening S., Hennig G., Eifel S., Gillner A., 2011. "Ultrafast Scan techniques for 3D-um Structuring of Metal Surfaces with high repetitive ps laser pulses," Physics Procedia 12, p.105